An Experimental and Mechanistic Modeling Study of Self-Initiated High-Temperature Polymerization of Ethyl Acrylate

Saeed Laki^{1†}, Ahmad A. Shamsabadi^{1†}, Hossein Riazi¹, Michael C. Grady², Andrew M. Rappe³, and Masoud Soroush^{1*}

¹Department of Chemical and Biological Engineering, Drexel University, Philadelphia, PA 19104

²Axalta Coating Systems, Global Innovation Center, Navy Yard, Philadelphia, PA 19112

November 6, 2019

REVISED VERSION

Submitted for Publication in the Special Issue of *Industrial and Engineering Chemistry**Research*, Christos Georgakis

Keywords: Free-radical polymerization, ethyl acrylate, monomer self-initiation, spontaneous thermal polymerization

³Department of Chemistry, University of Pennsylvania, Philadelphia, PA 19104

[†]These authors contributed equally to this work.

^{*} Corresponding author, Tel: +1-215-895-1710; E-mail: soroushm@drexel.edu

Abstract

High-temperature polymerization of acrylates involves numerous reactions. A reliable quantitative understanding of these reactions allows for producing high quality polymers, and for reliably designing, optimally operating, and intensifying the processes that produce the polymers. This paper presents an experimental and theoretical study of self-initiated thermal bulk polymerization of ethyl acrylate (EA) at 140, 160, 180, 200, and 220 °C. It reports kinetic parameter values for five important reactions of high-temperature EA homopolymerization. Before this study, only rate coefficients for secondary-radical propagation had been reported for EA. Guided by the family type behavior of acrylates, chain transfer to monomer from secondary and tertiary radicals, β -scission, backbiting, and monomer self-initiation reaction rate coefficients were estimated from measurements of monomer conversion and polymer average molecular weights. The resulting mechanistic model was found to predict monomer conversion and polymer average molecular weights satisfactorily over the wide temperature range. The estimated values of the EA self-initiation and chain-transfer-to-monomer reaction rate coefficients are in good agreement with those predicted by computational quantum chemistry.

1. Introduction

Ethyl acrylate (EA) is used as a monomer, a co-monomer, and a chemical intermediate for the synthesis of industrial products. Also, EA is used in the production of other chemicals such as dimethylaminoethyl acrylate¹, which has applications in pharmaceuticals, dental composites, surfactants, and water treatment agents²⁻⁴. Poly (ethyl acrylate) (PEA) is an industrially important polymer with low glass transition temperature, high elasticity, and excellent resistant against breakage. It is used in numerous applications such as water-based latex paints and coatings, construction and pressure-sensitive adhesives, coating for textiles, wood and paper processing, leather finishing resin, plastic manufacturing, non-woven fibers, and medical devices⁵⁻⁷.

The U.S. Environmental Protection Agency regulations has placed tight limits on the volatile organic components of paints and coatings, which has forced the industries to produce solvent-borne paints and coatings with a solvent content of less than 300 g·L⁻¹ ⁸⁻¹⁰. To ensure the brushability and sprayability^{8, 11} of these paints and coatings, these industries have had to lower the average molecular weights of polymers in their paints and coatings. High-temperature polymerization has been conducted widely to produce low-average molecular weight polymers¹². At high temperature, secondary reactions such as monomer self-initiation, β-scission, and inter/intra-molecular chain transfer contribute to polymerization appreciably^{11, 13-19}. Monomer self-initiation lowers the average molecular weights and decreases the need for conventional initiators in free-radical polymerization.

Reaction kinetics of acrylates in free radical polymerization strongly affect the properties of the final polymer products¹⁹. Rate coefficients of several reactions such as propagation and backbiting in free-radical polymerization of n-butyl acrylate (n-BA) were obtained through the

pulsed laser polymerization (PLP) technique²⁰⁻²². Recently, Vir et al.²³⁻²⁴ conducted high temperature PLP (below the boiling point of the monomer) to determine the β-scission reaction rate coefficient of n-BA. However, at very high temperatures (above the boiling point of the monomer) PLP may not yield an accurate value for the β-scission reaction rate coefficient²³⁻²⁸. In addition, molecular weight distributions (MWDs) of polymers have been analyzed using pulsed laser techniques and reversible addition-fragmentation chain transfer chain length-dependent termination (RAFT-CLD-T)²⁶ to determine the rate coefficient of free-radical propagation. The occurrence of intermolecular transfer to polymer reactions at high temperatures significantly lowered the accuracy of PLP-determined acrylate polymerization rate coefficients ^{19,29}.

The task of determining polymerization reaction mechanisms and kinetic parameter values can be helped with the use of techniques such as nuclear magnetic resonance (NMR) spectroscopy, matrix-assisted laser desorption ionization (MALDI)³⁰, spray ionization-Fourier transform mass spectroscopy, the free volume theory, and reversible addition-fragmentation chain transfer chain length-dependent termination (RAFT-CLD-T)²⁶. Other researchers have used a combination of experimental studies and mathematical modeling to determine the rate coefficient values ³¹⁻³³.

Electronic-level modeling (computational quantum chemistry)³⁴ has great potential for predicting reaction mechanisms and kinetic parameter values. Mechanistic modeling can also be used to estimate reaction kinetic parameters from measurements of monomer conversion and molecular weights, if reaction mechanisms and rate equations are all known. This latter approach was applied to estimate kinetic parameters of several reactions of methyl acrylate (MA) and *n*-BA^{10,35-36}. It was used to estimate frequency factors and activation energies of *n*-BA and MA self-initiation reactions from monomer conversion measurements ^{8,11}.

This paper presents an experimental and theoretical study of constant-temperature self-initiated thermal bulk polymerization of EA at 140, 160, 180, 200, and 220 °C, which are above the boiling point of EA. The theoretical study involves mechanistic modeling and reaction kinetic parameter estimation from measurements of monomer conversion and polymer average molecular weights. Before this study, for EA, only rate coefficients for secondary radical propagation had been reported. Furthermore, compared to other monomers, substantially much less experimental studies on EA have been reported. Based on the family type behavior (FTB) of alkyl acrylates, we first obtained reasonable ranges for unknown rate coefficients of EA chain transfer to monomer from secondary and tertiary radicals, β-scission, backbiting, and self-initiation reactions. These rate coefficients within the ranges were then estimated from the measurements. EA self-initiation and transfer-to-monomer rate coefficients are compared with the values predicted by computational quantum chemistry. The mechanistic model predictions of monomer conversion and polymer average molecular weights are also compared with measurements.

2. Experimental Procedures

EA monomer (>99.5%) stabilized with 20 ppm inhibitor (MEHQ|140-88-5 MFCD00009188) was purchased from ACROS Co. Stainless steel tubes with 4.8 mL capacity (L: 101.6 mm, ID: 7.0 mm, and OD: 9.0 mm) were used as batch mini reactors (Swagelok Inc., Huntingdon Valley, PA, USA). Both ends of the mini-reactor tubes were capped with stainless steel Swagelok caps, which can tolerate pressures up to 3,300 psig. Before polymerization, the monomer containing 20 ppm MEHQ was purified by passing it through an inhibitor removal column DHR-4 (Scientific Polymer Products of Ontario, New York), and the inhibitor-free EA

was collected in a glass flask. Before loading the mini-reactors with the monomer, the monomer in the glass flask capped with a rubber septum was bubbled with ultra-high purity nitrogen (>99.999%) for 4 hours to remove any trace of oxygen. To ensure that oxygen did not penetrate into the nitrogen-bubbled monomer through the septum, the glass flask was sealed with an aluminum foil, and the aluminum foil then was fixed with a rubber band. To load reactors with the monomer, a glove box (LC Technology Solution, Salisbury, USA) with an oxygen concentration of less than 1 ppm was used. First, all equipment, including the sealed flask containing nitrogen-bubbled EA, the reaction tubes, the caps and pipette, were purged by means of vacuum-nitrogen purge cycles. Second, the equipment was moved to the main chamber of the glove box to load the reactors with the monomer. Third, inside the glove box, 2.5 mL of the monomer was loaded into each reaction tube, and the caps were closed and tightened. Fourth, the loaded mini-reactors were weighed, and the weights were recorded. Fifth, two mini-reactors were placed inside a constant-temperature fluidized sand bath at the same time. The fluidized sand bath (Techne F946H SBL-2D manufactured by Alundum and Overspill Flange, USA) has an electrical heating element connected to a temperature controller. The desired sand bath temperature was set several hours before starting the polymerization to ensure that the sand bath has reached its steady-state temperature. The sand bath temperature monitored continuously and was found to vary within ±2 °C of the desired steady-state temperature. Our previous studies had shown that the temperature of the content of a mini-reactor reaches the sand bath temperature in about one minute 8, 11. A heat transfer analysis showed that the heat generated by EA polymerization is transferred to the sand very quickly due to the high thermal conductivity (18 J·K⁻¹.s⁻¹) of the alumina ceramic sand, the high air flow rate (35 cm·s⁻¹), the high thermal conductivity of the stainless walls of the mini-reactors³⁷⁻³⁸, and the high surface/volume ratio of the reactors. Sixth, the two tubes (mini-reactors) were taken out after a desired reaction time and were quenched rapidly in a cold-water bath. Seventh, when the temperature of the reactors reached the water bath temperature, each reactor was dried and weighed again to ensure that the reactor did not have any leakage during the reaction. In the case of a tube leakage, the tube was discarded, and the experiment was repeated. Eight, the content of each mini-reactor was emptied into a previously weighed aluminum dish. To remove unreacted monomer from the obtained polymers, the content of each reactor was dissolved in toluene and dried in a vacuum oven at 40 $^{\circ}$ C $^{8, 11, 17}$. Ninth, the gravimetric method was used to measure the conversion of monomer to polymer [Eq. S1, in Supporting Information (SI)] $^{8, 11}$. Tenth, number-average molecular weight (M_n) and weight-average molecular weight (M_w) of each sample were measured using gel permeation chromatography [Shimadzu High Performance Liquid Chromatography (LC-20AD)] with tetrahydrofuran as the mobile phase (SI).

3. Results and Discussion

3.1. Experimental Results

Self-initiated thermal polymerization of EA was conducted in the batch mini-reactors at constant temperatures of 140, 160, 180, 200, and 220 °C. Monomer conversion and molecular weights of the samples were measured at reaction times of 55, 110, 165, and 220 min at each temperature. Figures 1 shows that monomer conversion increases with temperature. At 140 and 160 °C after 220 min, the conversions of 0.008 and 0.028 were obtained, respectively. At 180 and 200 °C after 220 min, the conversion increases significantly to 0.217, 0.549, respectively, and at 220 °C to 0.8. Also, we conducted self-initiated thermal polymerization of EA at 120 °C. However, no conversion of monomer to polymer was observed at this temperature.

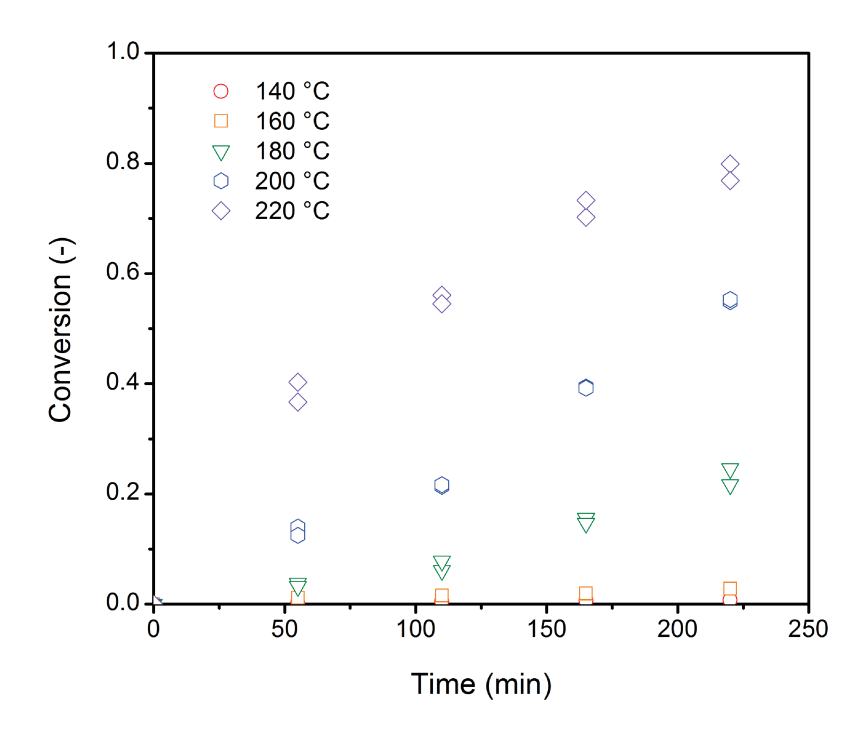


Figure 1. EA conversion measurements at 140, 160, 180, 200, and 220 °C.

Figure 2 shows M_n and M_w measurements of the polymer samples whose monomer conversion values are shown in Figure 1. As expected in free-radical polymerization, the average molecular weights decrease, as the reaction temperature increases. They also decreased slightly with reaction time. Figure 3 shows that the average molecular weights decreased sharply with monomer conversion at low conversions, but they decreased less with conversion at high conversions.

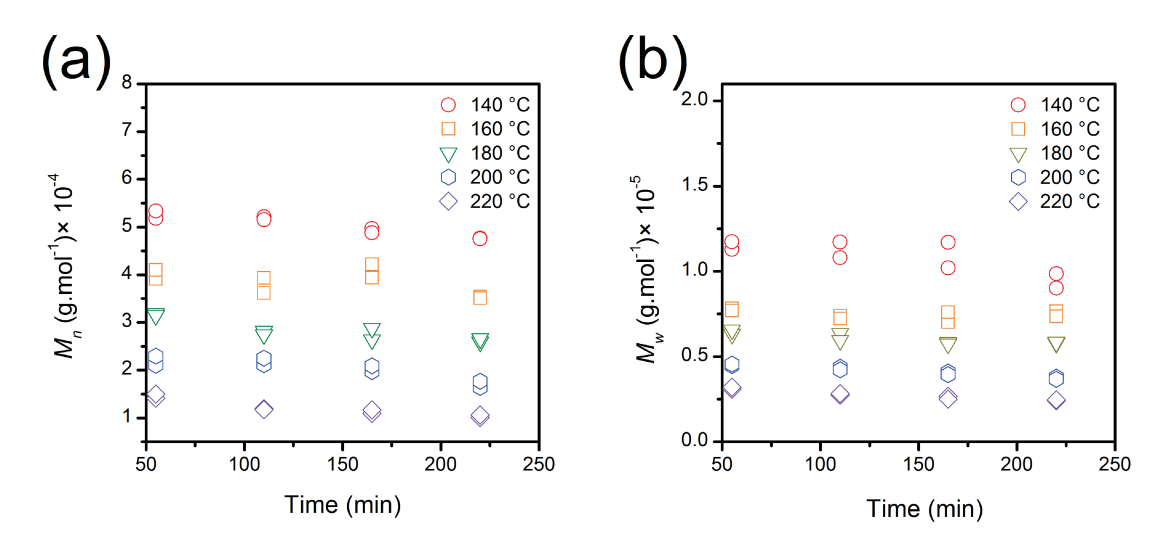


Figure 2. Measured PEA (a) M_n and (b) M_w at 140, 160, 180, 200, and 220 °C.

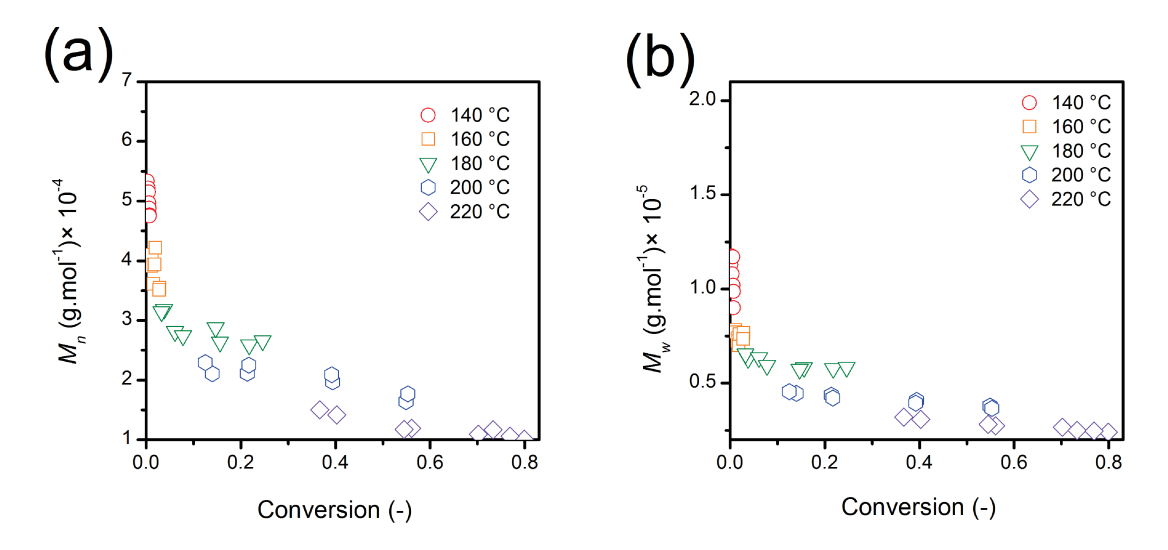


Figure 3. Measured PEA (a) M_n and (b) M_w versus measured EA conversion at 140, 160, 180, 200, and 220 °C.

3.2. Mechanistic Modeling

Many reactions occur in high-temperature polymerization of EA. These include monomer self-initiation, chain transfer to monomer, secondary and tertiary radicals chain propagation, inter-molecular chain transfer to polymer, termination by disproportionation, backbiting, β -scission, radical migration, and termination by combination ^{10, 18, 35-36, 39}. The kinetic parameter

values and rate equations for *n*-BA and MA polymerization reactions are given in Ref.^{8, 11, 39-40}. Acrylate monomers share significant similarities in terms of polymerization reactions. The same reactions occur in the free-radical polymerization of different members of the alkyl acrylate family.

For EA, only the activation energy and frequency factor of the secondary radical propagation $[2.69\times10^7 \text{ L}\cdot\text{mol}^{-1}.\text{s}^{-1}]$ and $[2.69\times10^7 \text{ L}\cdot\text{$

The following relationship between the tertiary and secondary propagation rate coefficients has been reported for the acrylates family ^{11,45}:

$$k_p^t = k_p \times 10^{-3} \tag{1}$$

where k_p is the secondary-radical propagation rate coefficient. Due to the unavailability of a reliable value for k_p^t of EA, we used Eq.1 and the EA secondary-radical propagation rate coefficient reported in Ref.^{30, 41} and calculated k_p^t for EA. Furthermore, for EA, no values have

been reported for the rate coefficients of the other reactions such as k_t (termination of secondary radicals), k_t^{tt} (termination of tertiary radicals), and $k_{tr,P}$ (chain-transfer-to-polymer). To address this problem, we invoked the FTB relationships^{11, 45} and estimated k_t , k_t^{tt} , and $k_{tr,P}$ rate coefficients. Furthermore, we used the FTB relationships to obtain initial estimation guesses for chain transfer to monomer from secondary and tertiary radicals, β -scission, and backbiting rate coefficients ($k_{tr,m}$, $k_{tr,m}^t$, k_{β} , and k_{bb} , respectively) and then searched for optimal estimates of k_{β} , k_{bb} , $k_{tr,m}$, and $k_{tr,m}^t$ within $\pm 20\%$ of their FTB values. For example, as $k_{p,EA}/k_{p,nBA}$ is close to one (0.91–0.93 at 413–493 K), we considered the FTB value of k_p for EA to be approximately equal to the k_p value for n-BA^{11, 45}, and searched for an optimal value of k_{bb} for EA between 80% and 120% of the k_{bb} value for n-BA.

The gel and glass effects play a significant role in bulk free-radical polymerization. At high monomer conversions, the viscosity of the reaction medium is very high, rendering propagation and termination reactions diffusion limited, and thus lowering propagation and termination reaction rates. To describe the effects of reaction-medium viscosity increase on the polymerization rate coefficients, several different models have been reported⁴⁶⁻⁴⁹. The glass transition temperatures of acrylates such as *n*-BA, EA and MA are very low (–53, –24 and 10 °C, respectively⁵⁰). Since the glass temperature (–24 °C) is lower than the reaction temperature (140–220 °C), the glass effect was not considered in this study⁵¹. However, the gel effect, which is reflective of the decline of apparent EA termination rate coefficients with increased reaction medium viscosity⁵²⁻⁵⁴, cannot be ignored⁵⁵⁻⁵⁷. To account for this drop in the apparent EA termination rate coefficients, we used the empirical gel effect model introduced in our previous work¹⁷:

$$k_{t_a} \cdot k_t^{-1} = \left(1 + \frac{A_1}{T + A_2} (e^{A_3 X} - 1)\right) \exp\left(\frac{-A_1}{T + A_2} (e^{A_3 X} - 1)\right)$$
 (2)

$$k_{t_a}^{tt} \cdot k_t^{tt-1} = \left(1 + \frac{A_1}{T + A_2} (e^{A_3 X} - 1)\right) \exp\left(\frac{-A_1}{T + A_2} (e^{A_3 X} - 1)\right)$$
(3)

where k_{t_a} and $k_{t_a}^{tt}$ are the apparent termination rate coefficients, and k_t and k_t^{tt} are the true termination rate coefficients. The model parameters $(A_1, A_2, \text{ and } A_3)$ depend on temperature linearly¹¹:

$$A_i = b_i + c_i T$$
, $i = 1, 2, 3$, $A_1 > 0$, $A_2 + T > 0$, $A_3 > 0$ (4)

where b_i and c_i are constants.

Given the set of acrylate polymerization reactions in Table 1 and the method of moments rate equations in Ref.⁵⁸, we derived ordinary differential equations that describe the dynamics of the batch mini-reactors.

To estimate the reaction kinetic and the gel-effect-model parameters from the monomer conversion, M_n and M_w measurements, the ordinary differential equations of the mechanistic model were integrated with MATLAB⁸. At each of the specific temperatures ($T_j = 140, 160, 180, 200, \text{ and } 220 \, ^{\circ}\text{C}$), $W_1, W_2, k_{i,m}, k_{tr,m}, k_{tr,m}^t, k_{bb}, k_{\beta}, A_1, A_2, \text{ and } A_3 \text{ were estimated by minimizing the following sum of squared relative residuals (SSRRs_j) using the <math>ga$ command of MATLAB¹¹:

$$SSRRs_{j} = \sum_{i=1}^{N_{j}} \left\{ W_{1,j} \times \left(\frac{X_{M}(t_{i},T_{j}) - X_{E}(t_{i},T_{j})}{X_{E}(t_{i},T_{j})} \right)^{2} + W_{2,j} \times \left(\frac{M_{n,M}(t_{i},T_{j}) - M_{n,E}(t_{i},T_{j})}{M_{n,E}(t_{i},T_{j})} \right)^{2} + (1 - W_{1,j} - W_{2,j}) \times \left(\frac{M_{w,M}(t_{i},T_{j}) - M_{w,E}(t_{i},T_{j})}{M_{w,E}(t_{i},T_{j})} \right)^{2} \right\}$$
(5)

where

$$X_{M}(t_{i}, T_{i}) = X_{Model}(t_{i}, T_{i}, k_{i,m}, k_{tr,m}, k_{tr,m}^{t}, k_{hh}, k_{hh}, k_{hh}, A_{1}, A_{2}, A_{3})$$

$$(6)$$

$$M_{n,M}(t_i, T_i) = M_{n,Model}(t_i, T_i, k_{i,m}, k_{tr,m}, k_{tr,m}^t, k_{bb}, k_{\beta}, A_1, A_2, A_3)$$
(7)

$$M_{w,M}(t_i, T_j) = M_{w,Model}(t_i, T_j, k_{i,m}, k_{tr,m}, k_{tr,m}^t, k_{bb}, k_{\beta}, A_1, A_2, A_3)$$
(8)

 $X_E(t_i, T_j)$, $M_{n,E}(t_i, T_j)$, and $M_{n,E}(t_i, T_j)$ are the experimental measurements of monomer conversion, M_n , and M_w at time t_i and temperature T_j , respectively. N_j is number of the samples, taken at temperature T_j . $W_{1,j}$ and $W_{2,j}$ are weights with:

$$0 < W_{1,j} < 1$$
, $0 < W_{2,j} < 1$, $0 < W_{1,j} + W_{2,j} < 1$.

 $X_M(t_i, T_j)$, $M_{n,M}(t_i, T_j)$ and $M_{w,M}(t_i, T_j)$ are, respectively, the values of conversion, M_n , and M_w at time t_i and temperature T_j predicted by the model with $k_{i,m}$, $k_{tr,m}$, $k_{tr,m}^t$, k_{bb} , k_{β} , A_1 , A_2 , and A_3 values.

The parameters $k_{i,m}$, $k_{tr,m}$, $k_{tr,m}^t$, k_{bb} , k_{β} , A_1 , A_2 , and A_3 were estimated from the measurements by following the steps:

- 1. $k_{i,m}$, $k_{tr,m}$, $k_{tr,m}^t$, k_{bb} , k_{β} , A_1 , A_2 , and A_3 at 140 °C were estimated via minimizing the SSRRs. The rate coefficient estimates were searched for within [80%, 120%] ranges of their corresponding FTB values (if applicable).
- 2. $k_{i,m}$, $k_{tr,m}$, $k_{tr,m}^t$, k_{bb} , k_{β} , A_1 , A_2 , and A_3 at 220 °C were estimated via minimizing the SSRRs. The rate coefficient estimates were searched for within [80%, 120%] ranges of their FTB values (if applicable).
- 3. The activation energy and frequency factor of each of the reactions were calculated from an Arrhenius plot of the 140 and 220 °C rate coefficients of the reaction.
- 4. $k_{l,m}$, $k_{tr,m}$, $k_{tr,m}^t$, k_{bb} , k_{β} , A_1 , A_2 , and A_3 at 160 °C were estimated via minimizing the SSRRs. The rate coefficient estimates were searched for within [80%, 120%] ranges of their 160°C values obtained from the Arrhenius equations obtained in Step 3.

Table 1. EA Self-Initiated Polymerization Reactions⁵⁸.

Table I. EA Self-Initiated Polymerization Reactions ³⁶ .					
Monomer self-initiation	Backbiting	Chain transfer to polymer			
$3M \stackrel{k_i}{\rightarrow} R_1^{**} + R_2^{**}$	$R_n^{**} \xrightarrow{k_{bb}} \tilde{R}_n^{***}$	$R_n^{**} + D_m \xrightarrow{m k_{tr,P}} D_n + R_m^{***}$			
		$R_n^{***} + D_m \xrightarrow{m k_{tr,P}^t} D_n + R_m^{***}$			
		$\tilde{R}_n^{***} + D_m \xrightarrow{mk_{tr,P}^t} D_n + R_m^{***}$			
Propagation	β-Scission	Termination by disproportionation			
$R_n^{**} + M \xrightarrow{\kappa_p} R_{n+1}^{**}$	$\tilde{R}_n^{***} \xrightarrow{\kappa_\beta} R_m^{**} + U_{n-m}$	$R_n^{**} + R_m^{**} \xrightarrow{k_{td}} D_n + U_m$			
$R_n^{***} + M \xrightarrow{k_p^{\prime}} R_{n+1}^{**}$	$\tilde{R}_n^{***} \stackrel{k_\beta}{\to} R_{n-m}^{**} + U_m$	$R_n^{**} + R_m^{**} \xrightarrow{k_{td}} D_m + U_n$			
$\tilde{R}_n^{***} + M \stackrel{k_p^t}{\rightarrow} R_{n+1}^{**}$	$R_n^{***} \xrightarrow{\kappa_\beta} R_m^{**} + U_{n-m}$	$R_n^{**} + R_m^{***} \xrightarrow{k_{td}^t} D_n + U_m$			
$R_n^{**} + U_m \xrightarrow{k_{mac}} R_{n+m}^{***}$	$R_n^{***} \xrightarrow{\kappa_\beta} R_{n-m}^{**} + U_m$	$R_n^{**} + R_m^{***} \xrightarrow{k_{td}^t} D_m + U_n$			
$R_n^{***} + U_m \xrightarrow{k_{mac}^{\overline{n}}} R_{n+m}^{***}$		$R_n^{**} + \tilde{R}_m^{***} \xrightarrow{k_{td}^t} D_m + U_n$			
$\tilde{R}_{n}^{***} + U_{m} \xrightarrow{k_{mac}^{t}} R_{n+m}^{***}$		$R_n^{**} + \tilde{R}_m^{***} \xrightarrow{k_{td}^t} D_n + U_m$			
		$R_n^{***} + R_m^{***} \xrightarrow{k_{td}^{tt}} D_n + U_m$			
		$R_n^{***} + R_m^{***} \xrightarrow{k_{td}^{tt}} D_m + U_n$			
		$R_n^{***} + \tilde{R}_m^{***} \xrightarrow{k_{td}^{tt}} D_m + U_n$			
		$R_n^{***} + \tilde{R}_m^{***} \xrightarrow{k_{td}^{tt}} D_n + U_m$			
		$\tilde{R}_n^{***} + \tilde{R}_m^{***} \xrightarrow{k_{td}^{tt}} D_n + U_m$			
		$\tilde{R}_n^{***} + \tilde{R}_m^{***} \xrightarrow{k_{td}^{tt}} D_m + U_n$			
Chain transfer to monomer	Termination	De-propagation			
$R_n^{**} + M \xrightarrow{k_{tr,m}} D_n + R_1^{**}$	by combination	$R_{n+1}^{**} \xrightarrow{k_{-p}} R_n^{**} + M$			
$R_n^{***} + M \xrightarrow{k_{tr,m}^t} D_n + R_1^{**}$	$R_n^{**} + R_m^{**} \xrightarrow{k_{tc}} D_{n+m}$ $2k_{tc}^t$				
$\tilde{R}_n^{***} + M \xrightarrow{k_{tr,m}^t} D_n + R_1^{**}$	$R_n^{**} + R_m^{***} \xrightarrow{2k_{tc}^t} D_{n+m}$				
	$R_n^{**} + \tilde{R}_m^{***} \xrightarrow{2k_{tc}^t} D_{n+m}$				
Chain transfer to macromonomer $(m-1)k_{rr,p}$	$R_n^{***} + R_m^{***} \xrightarrow{k_{tc}^{tt}} D_{n+m}$	Chain transfer to solvent $k_{tr,s}$			
$R_n^{**} + U_m \xrightarrow{(m-1)k_{tr,P}} D_n + R_m^{***}$	$R_n^{***} + \tilde{R}_m^{***} \xrightarrow{2k_{tc}^{tt}} D_{n+m}$	$R_n^{**} + S \xrightarrow{\kappa_{tr,s}} D_n + R_0^*$			
$R_n^{***} + U_m \xrightarrow{(m-1)k_{tr,P}^t} D_n + R_m^{***}$	$\tilde{R}_{n}^{***} + \tilde{R}_{m}^{***} \xrightarrow{k_{tc}^{tt}} D_{n+m}$	$R_n^{***} + S \xrightarrow[t]{k_{tr,s}^t} D_n + R_0^*$			
$\tilde{R}_n^{***} + U_m \xrightarrow{(m-1)k_{tr,P}^t} D_n + R_m^{***}$	n ne nem	$\tilde{R}_n^{***} + S \xrightarrow{k_{tr,s}^t} D_n + R_0^*$			

- 5. The same task of item 4 was conducted for 180 and 200 $^{\circ}$ C.
- 6. The final activation energy and frequency factor of each of the five reactions were calculated from an Arrhenius plot of the rate coefficient of each reaction at the five temperatures. Figure 4 shows an Arrhenius plot of the EA self-initiation reaction with $E_{i,m} = 187 \pm 2.4 \text{ kJ} \cdot \text{mol}^{-1}$ and, $\ln Z_{i,m} = 18.6 \pm 0.64 (Z_{i,m}, \text{L} \cdot \text{mol}^{-1} \cdot \text{s}^{-1})$. Arrhenius plots of

the other reactions are shown in Figures S1a-d of the SI. Table 2 presents the estimated five activation energies and five frequency factors. The estimates of the gel effect model parameters are presented in the Table 3, and the linear equations of the three parameters are:

$$A_1 = -0.315T + 215.340 (9)$$

$$A_2 = +0.130 \, T - 49.110 \tag{10}$$

$$A_3 = -0.060 T + 37.290 \tag{11}$$

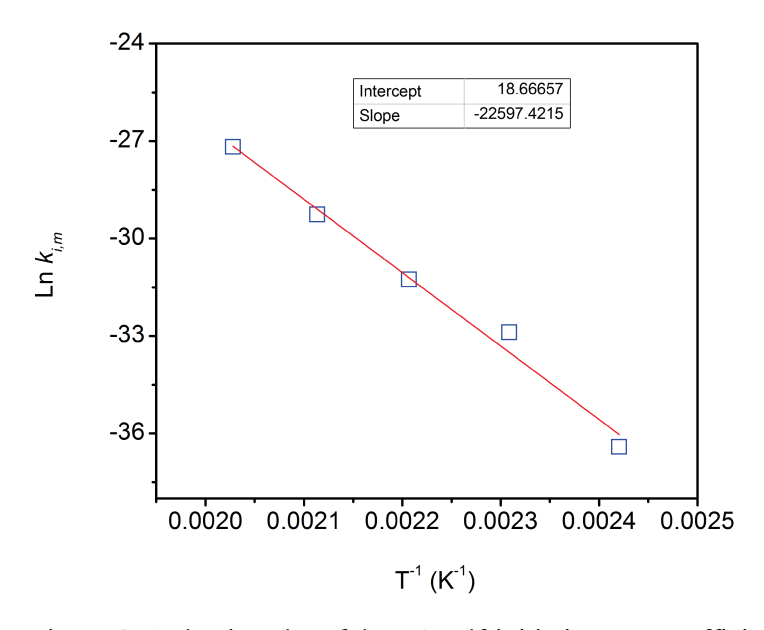


Figure 4. Arrhenius plot of the EA self-initiation rate coefficient.

Table 2. Kinetic parameters of the five EA polymerization reactions estimated in this work.

Rate Coefficient	Ln Z	E_a (kJ. mol ⁻¹)
k_{eta}	$32.2 \pm 0.49 \ (Z_{\beta}, s^{-1})$	91.4 ± 1.80
k_{bb}	$17.4 \pm 0.07 \ (Z_{bb}, \mathrm{s}^{-1})$	31.5 ± 0.29
$k_{tr,m}^t$	$5.8 \pm 0.02 \ (k_{tr,m}^t, \text{L·mol}^{-1}.\text{s}^{-1})$	32.6 ± 0.07
$k_{tr,m}$	$15.4 \pm 0.16 \ (k_{tr,m}, \text{L·mol}^{-1}.\text{s}^{-1})$	35.2 ± 0.61
$k_{i,m}$	$18.6 \pm 0.64 \ (Z_{i,m}, \text{L·mol}^{-1}.\text{s}^{-1})$	187.0 ± 2.40

Using density functional theory (DFT), our group had already studied the EA self-initiation and chain transfer to monomer reactions^{10, 34, 59-60}. Table 4 compares the estimates of the EA self-initiation rate coefficient at the five temperatures obtained in this work with the values predicted by computational quantum chemistry (PBE0/6-31G)⁶¹; it show that the mechanistic-model-estimated and the DFT predicted values agree well ^{10, 60}. Kinetic parameters of EA chain-transfer-to-monomer reaction had also been predicted using DFT with the B3LYP, X3LYP, and M06-2X functionals and the basis sets 6-31G(d), 6-31G(d,p), 6-311G(d) and 6-311G(d,p)^{10, 60}. The DFT predicted activation energies, frequency factors, and rate constants for these two EA-polymerization reactions are compared with the values estimated in this work in Tables 5. The table indicates that the estimates of chain-transfer-to-monomer rate coefficients obtained in this work are in good agreement with those predicted using M06-2X.

Table 3. Estimates of A_1 , A_2 , and A_3 at the five temperatures.

Temperature (°C)	140	160	180	200	220
<i>A</i> ₁ (K)	93.11	87.02	78.40	69.93	61.15
A_2 (K)	1.61	2.13	2.60	3.22	3.56
$A_3(-)$	6.21	5.33	4.20	3.14	2.42

Table 4. Comparison of EA self-initiation activation energies $(E_{i,m})$, frequency factors $(Z_{i,m})$, and rate coefficients $(k_{i,m})$ with values predicted by computational quantum chemistry (PBE0/6-31G)⁶¹.

	$E_{i,m}$	$\ln Z_{i,m}$	k	$_{i,m}$ (L·mol ⁻¹	.s ⁻¹) at Tem	perature (°C	C)
	(kJ mol ⁻¹)	$(Z_{i,m}, L \cdot \text{mol}^{-1}.s^{-1})$	140	160	180	200	220
PBE0/6-31G ⁶¹	115.0	1.0	2.5E-15	1.2E-14	4.8E-14	1.7E-13	5.8E-13
This work	187	18.7	1.5E-16	5.2E-15	2.7E-14	1.9E-13	1.5E-12

Table 5. Comparison of EA $E_{tr,m}$, $Z_{tr,m}$, and $k_{tr,m}$ estimates obtained in this work with predictions made by computational quantum chemistry (B3LYP/6-31G, X3LYP, and M06-2X) ¹⁰.

	Level of theory		$E_{tr,m}$		$k_{tr,m}$ at Temperatures (°C) (L·mol ⁻¹ .s ⁻¹)				
	Functional	Basis set			140	160	180	200	220
		6-31G(d)	56	12.57	0.02	0.05	0.10	0.20	0.34
	B3LYP 10	6-31G(d,p)	54	12.80	0.05	0.11	0.20	0.40	0.69
	DJL11	6-311G(d)	60	12.37	0.01	0.01	0.03	0.06	0.11
		6-311G(d,p)	57	12.78	0.02	0.05	0.10	0.20	0.33
		6-31G(d)	57	12.54	0.02	0.04	0.07	0.14	0.26
DFT	X3LYP 10	6-31G(d,p)	50	12.37	0.11	0.22	0.41	0.71	1.19
		6-311G(d)	56	12.25	0.02	0.04	0.07	0.14	0.24
		6-311G(d,p)	54	11.75	0.02	0.04	0.07	0.14	0.24
		6-31G(d,p)	41	11.75	0.83	1.44	2.40	3.78	5.76
	$M06-2X^{10}$	6-311G(d)	40	11.74	1.10	1.90	3.07	4.81	7.27
		6-311G(d,p)	44	11.78	0.36	0.65	1.11	1.81	2.85
	This work		35	15.40	2.06	3.25	4.91	7.17	10.17

Tables S1a-h (SI) compare the EA reaction kinetic parameter values obtained in this work for each of the five reactions with the lower and upper limits obtained for the same reactions using the FTB and parameter values reported in Ref. $^{16, 28, 39-40, 45, 62-66}$. As it was required in the constrained parameter estimation, the EA rate coefficient values obtained in this study are within $\pm 20\%$ of their nominal FTB values at 140, 160, 180, 200, and 220 °C.

Figures 5, 6 and 7 compare model-predictions and measurements of conversion and the average molecular weights. They indicate that the model can predict the properties accurately within the wide temperature and time ranges. Figure 8 shows the best conversion predictions that without and with the gel effect model, the mechanistic model can make at 220 °C. The prediction

without the gel effect model was obtained with kinetic parameter estimates that minimized the sum of the relative residuals in the absence of the gel effect model, while the other prediction was obtained with kinetic parameter estimates that minimized the sum of the relative residuals in the presence of the gel effect model. It is clear that the mechanistic model without the gel effect model is unable to predict reliably even with the optimal adjustment of the reaction rate coefficients. Figure 9 shows how the $k_{t_a} \cdot k_t^{-1}$ ratio described by the gel effect model with the A₁, A₂ and A₃ estimates, varies with temperature and monomer conversion. As monomer conversion increases (temperature increases), the $k_{t_a} \cdot k_t^{-1}$ ratio decreases (increases) monotonously.

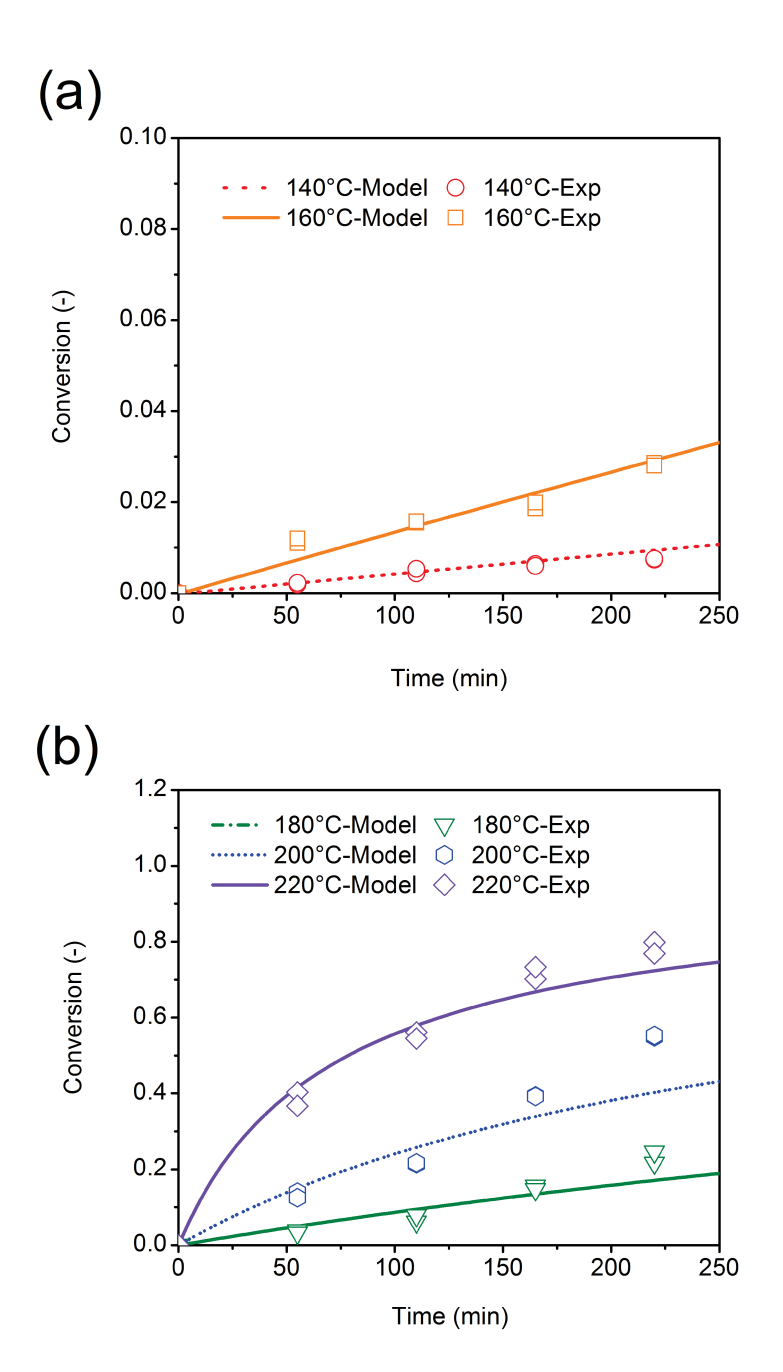


Figure 5. Predicted and measured EA conversion at the temperatures.

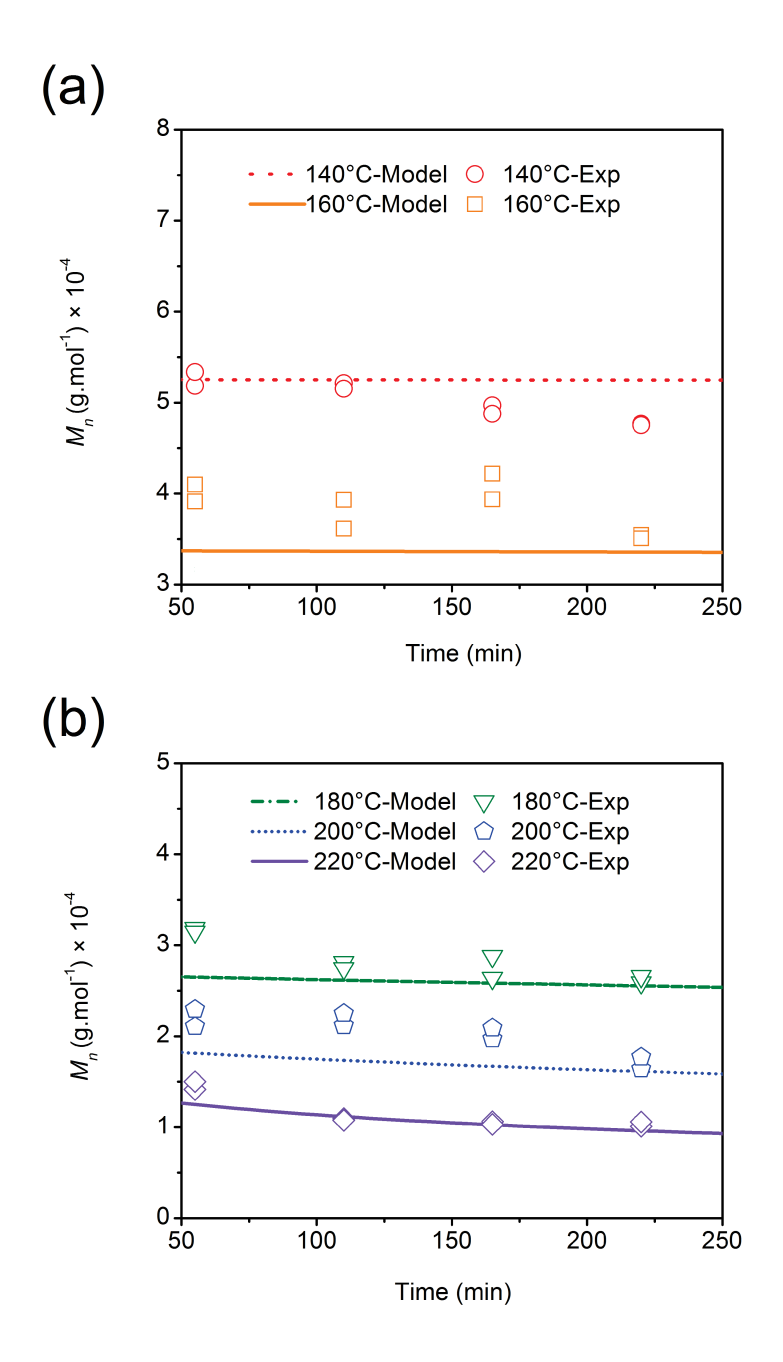
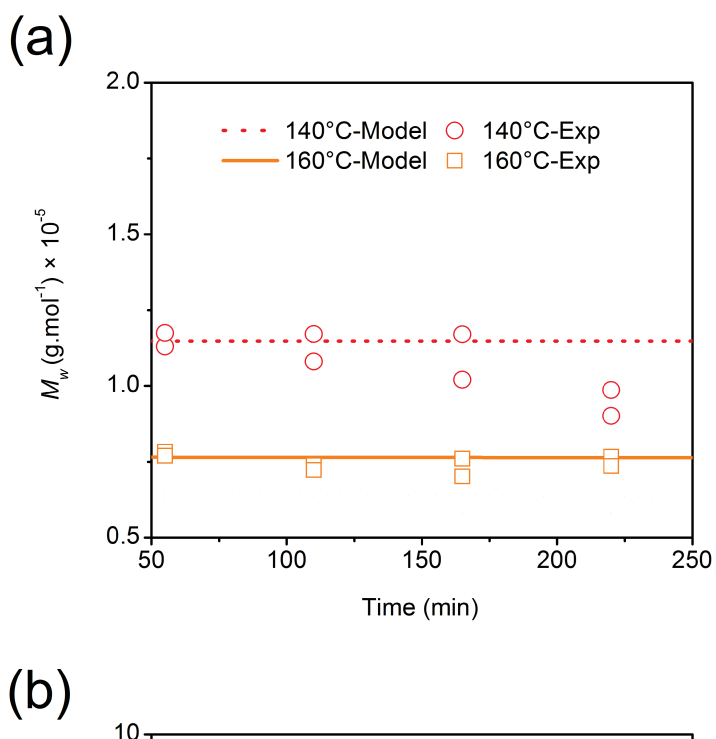


Figure 6. Predicted and measured PEA number-average molecular weights at the temperatures.



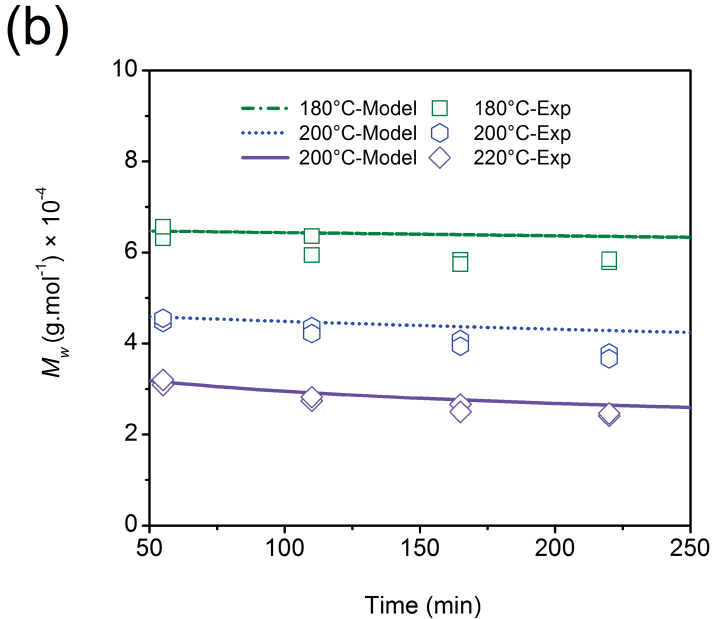


Figure 7. Predicted and measured PEA weight-average molecular weights at the temperatures.

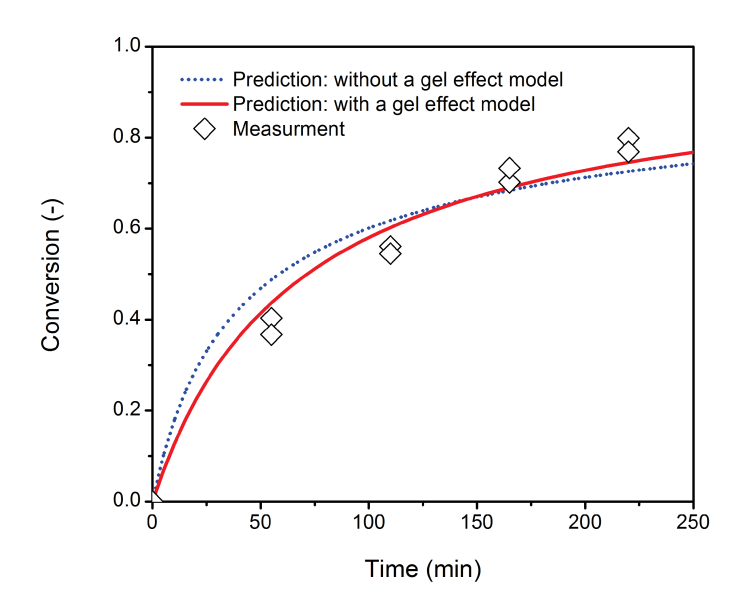


Figure 8. Mechanistic-model predictions of EA conversion with and without the gel effect model at 220 $^{\circ}\mathrm{C}.$

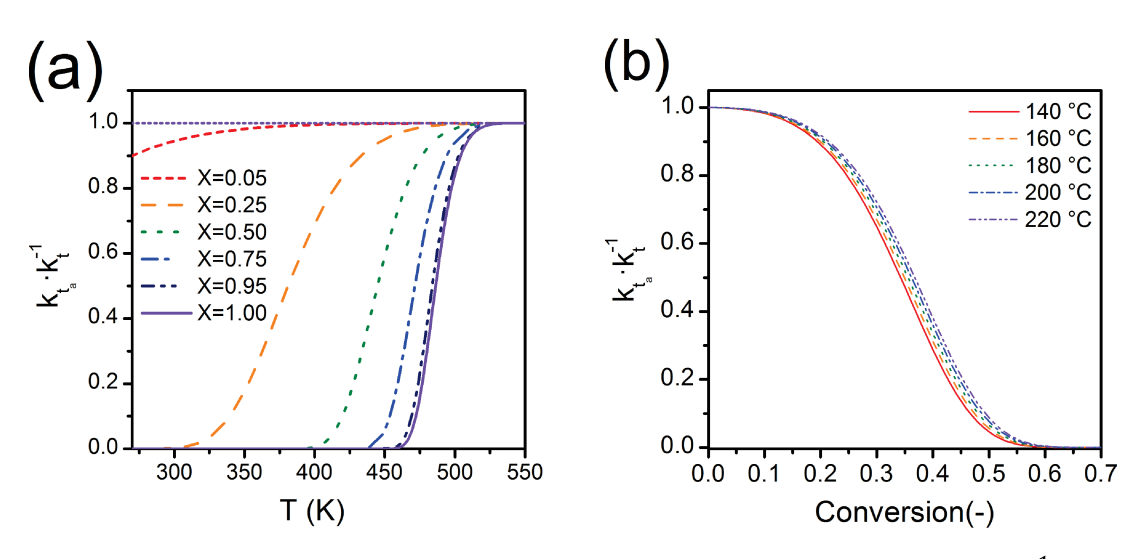


Figure 9. Effects of temperature and monomer conversion on the $k_{t_a} \cdot k_t^{-1}$ ratio.

4. Conclusions

Self-initiated thermal bulk polymerization of EA was carried out in mini-batch reactors at constant temperatures of 140, 160, 180, 200, and 220 °C. The monomer conversion and polymer average molecular weights were measured at different reaction times and temperatures. Kinetic parameters of the five EA polymerization reactions were estimated from monomer conversion and polymer average molecular weights measurements. In view that eight parameters were estimated at each temperature, and β-scission and backbiting are series reactions, these parameter estimates were constrained to the ranges obtained from the family type behavior of acrylates. The mechanistic polymerization reactor model was found to predict the polymer properties satisfactorily. In addition, the estimated values of the rate coefficients of the EA self-initiation and chain transfer to monomer reactions were found to be in good agreement with the values predicted by computational quantum chemistry. The kinetic parameter values obtained in this study enable simulation of polymerization processes, which use EA as a monomer or comonomer. The reliable quantitative understanding of the EA polymerization reactions allows for designing and producing high quality polymers using intensified processes with optimal operating conditions.

Acknowledgement

This material is based upon work supported by the U.S. National Science Foundation under Grant Nos. CBET–1804285 and CBET–1803215. Any opinions, findings, and conclusions or recommendations expressed in this material are those of the authors and do not necessarily reflect the views of the National Science Foundation

Acronyms

DFT	Density functional theory
EA	Ethyl acrylate
FTB	Family type behavior
FRP	Free-radical polymerization
n-BA	Normal butyl acrylate
MA	Methyl acrylate
MWD	Molecular weight distribution
MALDI	Matrix-assisted laser desorption ionization
NMR	Nuclear magnetic resonance
PLP	Pulsed laser polymerization

Notations

Symbol	Unit	Definition
A_1	K	Gel effect model parameter
A_2	K	Gel effect model parameter
A_3	-	Gel effect model parameter
$E_{i,m}$	kJ·mol⁻¹	Activation energy of reaction <i>i</i>
k_p	L.mol ⁻¹ .s ⁻¹	Secondary radical propagation rate coefficient
k_p^t	L.mol ⁻¹ .s ⁻¹	Tertiary radical propagation rate coefficient
k_t	L.mol ⁻¹ .s ⁻¹	Termination by secondary radicals
k_t^{tt}	L.mol ⁻¹ .s ⁻¹	Termination by tertiary radicals
k_eta	s ⁻¹	β-scission rate coefficient
k_{bb}	s ⁻¹	Backbiting rate coefficient
$k_{tr,m}$	L.mol ⁻¹ .s ⁻¹	Transfer-to-monomer from secondary radical
$k_{tr,m}^t$	L.mol ⁻¹ .s ⁻¹	Transfer-to-monomer from tertiary radical
$k_{i,m}$	mol ⁻¹ .s ⁻¹	Self-initiation rate coefficient
k_{t_a}	L.mol ⁻¹ .s ⁻¹	Apparent termination rate coefficients by secondary radicals
$k_{t_a}^{tt}$	L.mol ⁻¹ .s ⁻¹	Apparent termination rate coefficients by tertiary radicals
M_n	g.mol ⁻¹	Number-average molecular weight
M_{w}	g.mol ⁻¹	Weight-average molecular weight
$M_{n,E}$	g.mol ⁻¹	Measurement of M_n
$M_{w,E}$	g.mol ⁻¹	Measurement of M_w
$M_{n,M}$	g.mol ⁻¹	Model-predicted M_n
$M_{w,M}$	g.mol ⁻¹	Model-predicted M_w
N_j	-	Number of polymer samples
t_i	min	Sampling time instant
T_j	K	Temperature

W_1	-	Weight factor
W_2	-	Weight factor
X_E	-	Measurement of monomer conversion
Z_i	-	Frequency factor of reaction <i>i</i>

Supporting Information

Gravimetric Method

Molecular Weights Measurements

Figure S1. The GPC calibration curve.

Figure S2. Arrhenius plots of (a) k_{β} , (b) k_{bb} , (c) $k_{tr.m}$, and (d) $k_{tr.m}^t$.

Table S1a. Comparison of the estimates of EA k_{bb} , (s⁻¹) obtained in this study with the minimum and maximum values of EA k_{bb} obtained from FTB.

Table S1b. Comparison of the estimates of EA k_{β} (s⁻¹) obtained in this study with the minimum and maximum values of EA k_{β} obtained from FTB.

Table S1c. Comparison of the estimates of EA $k_{tr,m}$ (L.mol⁻¹.s⁻¹) obtained in this study with the minimum and maximum values of EA $k_{tr,m}$ obtained from FTB.

Table S1d. Comparison of the estimates of EA $k_{tr,m}^t$ (L.mol⁻¹.s⁻¹) obtained in this study with the minimum and maximum values of EA $k_{tr,m}^t$ obtained from FTB.

Table S1e. Comparison of the estimates of EA k_t (L.mol⁻¹.s⁻¹) obtained from FTB and used in this study with the minimum and maximum values of EA k_t obtained from FTB.

Table S1f. Comparison of the estimates of EA k_t^{tt} (L.mol⁻¹.s⁻¹) obtained from FTB and used in this study with the minimum and maximum values of EA k_t^{tt} obtained from FTB.

Table S1g. Comparison of the estimates of EA k_p^t (L.mol⁻¹.s⁻¹) obtained from FTB and used in this study with the minimum and maximum values of EA k_p^t obtained from FTB.

Table S1h. Comparison of the estimates of EA $k_{tr,P}$ (L.mol⁻¹.s⁻¹) obtained from FTB and used in this study with the minimum and maximum values of EA $k_{tr,P}$ obtained from FTB.

References

- 1. Sideridou-Karayannidou, I.; Seretoudi, G., Synthesis and characterization of copolymers of N-vinylcarbazole and N, N-dimethylaminoethyl acrylate. *Polymer* **1999**, *40* (17), 4915-4922.
- 2. Denyer, R.; Fortuin, M. S., Dental compositions from urethane acrylate, diacrylate monomer, camphorquinone and dimethylaminoethyl methacrylate. Google Patents: 1984.
- 3. Bian, K.; Cunningham, M. F., Surface-initiated nitroxide-mediated radical polymerization of 2-(dimethylamino) ethyl acrylate on polymeric microspheres. *Polymer* **2006**, *47* (16), 5744-5753.
- 4. Alexandridis, P.; Lindman, B., Amphiphilic block copolymers: self-assembly and applications. Elsevier: 2000.
- 5. Dittgen, M.; Durrani, M.; Lehmann, K., *Acrylic polymers A review of pharmaceutical applications*. 1997; Vol. 7, p 403-437.
- 6. Ohara, T.; Sato, T.; Shimizu, N.; Prescher, G.; Schwind, H.; Weiberg, O.; Marten, K.; Greim, H., Acrylic acid and derivatives. *Ullmann's encyclopedia of industrial chemistry* **2003**.
- 7. Datta, H.; Bhowmick, A. K.; Singha, N. K. In *Atom transfer radical polymerization (ATRP) of ethyl acrylate: Its mechanistic studies*, Macromolecular symposia, Wiley Online Library: 2006; pp 245-251.
- 8. Arabi Shamsabadi, A.; Moghadam, N.; Srinivasan, S.; Corcoran, P.; Grady, M. C.; Rappe, A. M.; Soroush, M., Study of n-Butyl Acrylate Self-Initiation Reaction Experimentally and via Macroscopic Mechanistic Modeling. *Processes* **2016**, *4* (2), 15.
- 9. VOC's Directive, E., committee of the American chamber of commerce in Belgium, ASBL/VZw, Brussels, July 8, 1996. *There is no corresponding record for this reference.*[Google Scholar].
- 10. Moghadam, N.; Liu, S.; Srinivasan, S.; Grady, M. C.; Soroush, M.; Rappe, A. M., Computational study of chain transfer to monomer reactions in high-temperature polymerization of alkyl acrylates. *The Journal of Physical Chemistry A* **2013**, *117* (12), 2605-2618.
- 11. Riazi, H.; A. Shamsabadi, A.; Grady, M. C.; Rappe, A. M.; Soroush, M., Experimental and Theoretical Study of the Self-Initiation Reaction of Methyl Acrylate in Free-Radical Polymerization. *Industrial & Engineering Chemistry Research* **2018**, *57* (2), 532-539.
- 12. Campbell, J.; Teymour, F.; Morbidelli, M., High temperature free radical polymerization. 1. Investigation of continuous styrene polymerization. *Macromolecules* **2003**, *36* (15), 5491-5501.
- 13. Cooper, G.; Grieser, F.; Biggs, S., Butyl acrylate/vinyl acetate copolymer latex synthesis using ultrasound as an initiator. *Journal of colloid and interface science* **1996**, *184* (1), 52-63.
- 14. Nason, C.; Roper, T.; Hoyle, C.; Pojman, J. A., UV-Induced frontal polymerization of multifunctional (meth) acrylates. *Macromolecules* **2005**, *38* (13), 5506-5512.
- 15. Hui, A. W.; Hamielec, A. E., Thermal polymerization of styrene at high conversions and temperatures. An experimental study. *Journal of Applied Polymer Science* **1972**, *16* (3), 749-769.
- 16. Arzamendi, G.; Plessis, C.; Leiza, J. R.; Asua, J. M., Effect of the intramolecular chain transfer to polymer on PLP/SEC experiments of alkyl acrylates. *Macromolecular theory and simulations* **2003**, *12* (5), 315-324.

- 17. Riazi, H.; Shamsabadi, A. A.; Corcoran, P.; Grady, M. C.; Rappe, A. M.; Soroush, M., On the Thermal Self-Initiation Reaction of n-Butyl Acrylate in Free-Radical Polymerization. *Processes* **2018**, *6* (1), 3.
- 18. Quan, C.; Soroush, M.; Grady, M. C.; Hansen, J. E.; Simonsick, W. J., High-temperature homopolymerization of ethyl acrylate and n-butyl acrylate: Polymer characterization. *Macromolecules* **2005**, *38* (18), 7619-7628.
- 19. Junkers, T.; Barner-Kowollik, C., The role of mid-chain radicals in acrylate free radical polymerization: Branching and scission. *Journal of Polymer Science Part A: Polymer Chemistry* **2008**, *46* (23), 7585-7605.
- 20. Beuermann, S.; Buback, M.; Davis, T. P.; Gilbert, R. G.; Hutchinson, R. A.; Olaj, O. F.; Russell, G. T.; Schweer, J.; van Herk, A. M., Critically evaluated rate coefficients for free-radical polymerization, 2.. Propagation rate coefficients for methyl methacrylate. *Macromolecular Chemistry and Physics* **1997**, *198* (5), 1545-1560.
- 21. Beuermann, S.; Buback, M.; Davis, T. P.; Gilbert, R. G.; Hutchinson, R. A.; Kajiwara, A.; Klumperman, B.; Russell, G. T., Critically evaluated rate coefficients for free-radical polymerization, 3. Propagation rate coefficients for alkyl methacrylates. *Macromolecular Chemistry and Physics* **2000**, *201* (12), 1355-1364.
- 22. Willemse, R. X.; van Herk, A. M.; Panchenko, E.; Junkers, T.; Buback, M., PLP– ESR Monitoring of Midchain Radicals in n-Butyl Acrylate Polymerization. *Macromolecules* **2005**, *38* (12), 5098-5103.
- 23. Vir, A. B.; Marien, Y.; Van Steenberge, P. H.; Barner-Kowollik, C.; Reyniers, M.-F.; Marin, G. B.; D'hooge, D. R., Access to the β -scission rate coefficient in acrylate radical polymerization by careful scanning of pulse laser frequencies at elevated temperature. *Reaction Chemistry & Engineering* **2018**, *3* (5), 807-815.
- 24. Vir, A. B.; Marien, Y.; Van Steenberge, P.; Barner-Kowollik, C.; Reyniers, M.-F.; Marin, G. B.; D'hooge, D. R., From n-Butyl Acrylate Arrhenius Parameters for Backbiting and Tertiary Propagation to β-scission via Stepwise Pulsed Laser Polymerization. *Polymer Chemistry* **2019**.
- 25. Hamzehlou, S.; Ballard, N.; Reyes, Y.; Aguirre, A.; Asua, J.; Leiza, J., Analyzing the discrepancies in the activation energies of the backbiting and β -scission reactions in the radical polymerization of n-butyl acrylate. *Polymer Chemistry* **2016**, *7* (11), 2069-2077.
- 26. Barth, J.; Buback, M.; Hesse, P.; Sergeeva, T., Termination and transfer kinetics of butyl acrylate radical polymerization studied via SP-PLP-EPR. *Macromolecules* **2010**, *43* (9), 4023-4031.
- 27. Plessis, C.; Arzamendi, G.; Leiza, J.; Schoonbrood, H.; Charmot, D.; Asua, J., A decrease in effective acrylate propagation rate constants caused by intramolecular chain transfer. *Macromolecules* **2000**, *33* (1), 4-7.
- 28. Kattner, H.; Buback, M., Termination, Propagation, and Transfer Kinetics of Midchain Radicals in Methyl Acrylate and Dodecyl Acrylate Homopolymerization. *Macromolecules* **2017**, *51* (1), 25-33.
- 29. Barner-Kowollik, C.; Russell, G. T., Chain-length-dependent termination in radical polymerization: Subtle revolution in tackling a long-standing challenge. *Progress in Polymer Science* **2009**, *34* (11), 1211-1259.

- 30. Willemse, R.; Van Herk, A., Determination of propagation rate coefficients of a family of acrylates with PLP-MALDI-ToF-MS. *Macromolecular Chemistry and Physics* **2010**, *211* (5), 539-545.
- 31. Pritchard, D. J.; Bacon, D. W., Prospects for reducing correlations among parameter estimates in kinetic models. *Chemical Engineering Science* **1978**, *33* (11), 1539-1543.
- 32. Brandolin, A.; Capiati, N. J.; Farber, J. N.; Valles, E. M., Mathematical model for high-pressure tubular reactor for ethylene polymerization. *Industrial & engineering chemistry research* **1988**, *27* (5), 784-790.
- 33. Wang, W.; Hutchinson, R. A.; Grady, M. C., Study of butyl methacrylate depropagation behavior using batch experiments in combination with modeling. *Industrial & Engineering Chemistry Research* **2009**, *48* (10), 4810-4816.
- 34. Soroush, M., *Computational Quantum Chemistry: Insights into Polymerization Reactions*. Elsevier: 2019.
- 35. Srinivasan, S.; Lee, M. W.; Grady, M. C.; Soroush, M.; Rappe, A. M., Computational study of the self-initiation mechanism in thermal polymerization of methyl acrylate. *The Journal of Physical Chemistry A* **2009**, *113* (40), 10787-10794.
- 36. Liu, S.; Srinivasan, S.; Grady, M. C.; Soroush, M.; Rappe, A. M., Computational study of cyclohexanone–monomer co-initiation mechanism in thermal homo-polymerization of methyl acrylate and methyl methacrylate. *The Journal of Physical Chemistry A* **2012**, *116* (22), 5337-5348.
- 37. Moore, J. S.; Jensen, K. F., "Batch" kinetics in flow: online IR analysis and continuous control. *Angewandte Chemie International Edition* **2014**, *53* (2), 470-473.
- 38. Bally, F.; Serra, C. A.; Hessel, V.; Hadziioannou, G., Homogeneous polymerization: benefits brought by microprocess technologies to the synthesis and production of polymers. *Macromolecular Reaction Engineering* **2010**, *4* (9-10), 543-561.
- 39. Maeder, S.; Gilbert, R. G., Measurement of transfer constant for butyl acrylate free-radical polymerization. *Macromolecules* **1998**, *31* (14), 4410-4418.
- 40. Derboven, P.; D'hooge, D. R.; Reyniers, M.-F.; Marin, G. B.; Barner-Kowollik, C., The long and the short of radical polymerization. *Macromolecules* **2015**, *48* (3), 492-501.
- 41. van Herk, A. M., Historic account of the development in the understanding of the propagation kinetics of acrylate radical polymerizations. *Macromolecular rapid communications* **2009**, *30* (23), 1964-1968.
- 42. Bamford, C.; Dyson, R.; Eastmond, G., Network formation IV. The nature of the termination reaction in free-radical polymerization. *Polymer* **1969**, *10*, 885-899.
- 43. Fehéarvári, A.; Földes-Berezsnich, T.; Tüdös, F., Kinetics of radical polymerization. XXIX. Kinetics of initiation in the polymerization of ethyl acrylate. *Journal of Macromolecular Science—Chemistry* **1980**, *14* (7), 1071-1084.
- 44. Ballard, N.; Asua, J. M., Radical polymerization of acrylic monomers: An overview. *Progress in Polymer Science* **2017**.
- 45. Barner-Kowollik, C.; Beuermann, S.; Buback, M.; Castignolles, P.; Charleux, B.; Coote, M. L.; Hutchinson, R. A.; Junkers, T.; Lacík, I.; Russell, G. T., Critically evaluated rate coefficients in radical polymerization—7. Secondary-radical propagation rate coefficients for methyl acrylate in the bulk. *Polymer Chemistry* **2014**, *5* (1), 204-212.

- 46. Chiu, W. Y.; Carratt, G. M.; Soong, D. S., A computer model for the gel effect in free-radical polymerization. *Macromolecules* **1983**, *16* (3), 348-357.
- 47. Schmidt, A. D.; Ray, W. H., The dynamic behavior of continuous polymerization reactors—I: Isothermal solution polymerization in a CSTR. *Chemical Engineering Science* **1981**, *36* (8), 1401-1410.
- 48. Tulig, T. J.; Tirrell, M., Molecular theory of the Trommsdorff effect. *Macromolecules* **1981**, *14* (5), 1501-1511.
- 49. Achilias, D. S., A review of modeling of diffusion controlled polymerization reactions. *Macromolecular theory and simulations* **2007**, *16* (4), 319-347.
- 50. Gao, J.; McManus, N. T.; Penlidis, A., Experimental and simulation studies on ethyl acrylate polymerization. *Macromolecular Chemistry and Physics* **1997**, *198* (3), 843-859.
- 51. Tefera, N.; Weickert, G.; Westerterp, K., Modeling of free radical polymerization up to high conversion. I. A method for the selection of models by simultaneous parameter estimation. *Journal of Applied Polymer Science* **1997**, *63* (12), 1649-1661.
- 52. Beuermann, S.; Buback, M., Rate coefficients of free-radical polymerization deduced from pulsed laser experiments. *Progress in Polymer Science* **2002**, *27* (2), 191-254.
- 53. Gao, J.; Penlidis, A., A comprehensive simulator/database package for reviewing free-radical homopolymerizations. *Journal of Macromolecular Science, Part C: Polymer Reviews* **1996,** *36* (2), 199-404.
- 54. Matheson, M. S.; Auer, E.; Bevilacqua, E. B.; Hart, E., Rate Constants in Free Radical Polymerizations. IV. Methyl Acrylate. *Journal of the American Chemical Society* **1951**, *73* (11), 5395-5400.
- 55. Matyjaszewski, K.; Davis, T. P., *Handbook of radical polymerization*. John Wiley & Sons: 2003.
- 56. Buback, M.; Egorov, M.; Feldermann, A., chain-length dependence of termination rate coefficients in acrylate and methacrylate homopolymerizations investigated via the SP- PLP technique. *Macromolecules* **2004**, *37* (5), 1768-1776.
- 57. Theis, A.; Feldermann, A.; Charton, N.; Stenzel, M. H.; Davis, T. P.; Barner-Kowollik, C., Access to Chain Length Dependent Termination Rate Coefficients of Methyl Acrylate via Reversible Addition– Fragmentation Chain Transfer Polymerization. *Macromolecules* **2005**, *38* (7), 2595-2605.
- 58. Riazi, H.; Arabi Shamsabadi, A.; Grady, M. C.; Rappe, A. M.; Soroush, M., Method of Moments Applied to the Most-Likely High-Temperature Free-Radical Polymerization Reactions. *Processes* **2019**, *7* (10), 656.
- 59. Srinivasan, S.; Lee, M. W.; Grady, M. C.; Soroush, M.; Rappe, A. M., Self-initiation mechanism in spontaneous thermal polymerization of ethyl and n-butyl acrylate: A theoretical study. *The Journal of Physical Chemistry A* **2010**, *114* (30), 7975-7983.
- 60. Moghadam, N.; Liu, S.; Srinivasan, S.; Grady, M. C.; Rappe, A. M.; Soroush, M., Theoretical study of intermolecular chain transfer to polymer reactions of alkyl acrylates. *Industrial & Engineering Chemistry Research* **2015**, *54* (16), 4148-4165.
- 61. Liu, S.; Srinivasan, S.; Tao, J.; Grady, M. C.; Soroush, M.; Rappe, A. M., Modeling spin-forbidden monomer self-initiation reactions in spontaneous free-radical polymerization of acrylates and methacrylates. *The Journal of Physical Chemistry A* **2014**, *118* (40), 9310-9318.

- 62. Buback, M.; Kuelpmann, A.; Kurz, C., Termination kinetics of methyl acrylate and dodecyl acrylate free-radical homopolymerizations up to high pressure. *Macromolecular Chemistry and Physics* **2002**, *203* (8), 1065-1070.
- 63. Brandrup, J.; Immergut, E.; Grulke, E.; Abe, A.; Bloch, D., Handbook of polymers. John Wiley & Sons, New York: 1989.
- 64. Nikitin, A. N.; Hutchinson, R. A.; Kalfas, G. A.; Richards, J. R.; Bruni, C., The Effect of Intramolecular Transfer to Polymer on Stationary Free-Radical Polymerization of Alkyl Acrylates, 3—Consideration of Solution Polymerization up to High Conversions. *Macromolecular Theory and Simulations* **2009**, *18* (4-5), 247-258.
- 65. Nikitin, A. N.; Hutchinson, R. A.; Wang, W.; Kalfas, G. A.; Richards, J. R.; Bruni, C., Effect of Intramolecular Transfer to Polymer on Stationary Free-Radical Polymerization of Alkyl Acrylates, 5–Consideration of Solution Polymerization up to High Temperatures. *Macromolecular Reaction Engineering* **2010**, *4* (11-12), 691-706.
- 66. Sun, Q.; Aguila, B.; Perman, J.; Earl, L. D.; Abney, C. W.; Cheng, Y.; Wei, H.; Nguyen, N.; Wojtas, L.; Ma, S., Postsynthetically modified covalent organic frameworks for efficient and effective mercury removal. *Journal of the American Chemical Society* **2017**, *139* (7), 2786-2793.